Extrahepatic deficiency of transferrin receptor 2 is associated with increased erythropoiesis independent of iron overload

Received for publication, August 6, 2019, and in revised form, February 11, 2020 Published, Papers in Press, February 13, 2020, DOI 10.1074/jbc.RA119.010535

Aaron M. Wortham[‡], **Devorah C. Goldman**[§], **Juxing Chen**[‡1], **William H. Fleming**[§], **An-Sheng Zhang**[‡], and **Caroline A. Enns**[‡2]

From the Departments of [‡]*Cell, Developmental and Cancer Biology and* [§]*Pediatrics, Oregon Health and Science University, Portland, Oregon 97239*

Edited by F. Peter Guengerich

Transferrin receptor 2 (TFR2) is a transmembrane protein expressed mainly in hepatocytes and in developing erythroid cells and is an important focal point in systemic iron regulation. Loss of TFR2 function results in a rare form of the iron-overload disease hereditary hemochromatosis. Although TFR2 in the liver has been shown to be important for regulating iron homeostasis in the body, TFR2's function in erythroid progenitors remains controversial. In this report, we analyzed TFR2-deficient mice in the presence or absence of iron overload to distinguish between the effects caused by a high iron load and those caused by loss of TFR2 function. Analysis of bone marrow from TFR2-deficient mice revealed a reduction in the early burst-forming unit–erythroid and an expansion of late-stage erythroblasts that was independent of iron overload. Spleens of TFR2-deficient mice displayed an increase in colony-forming unit–erythroid progenitors and in all erythroblast populations regardless of iron overload. This expansion of the erythroid compartment coincided with increased erythroferrone (ERFE) expression and serum erythropoietin (EPO) levels. Rescue of hepatic TFR2 expression normalized hepcidin expression and the total cell count of the bone marrow and spleen, but it had no effect on erythroid progenitor frequency. On the basis of these results, we propose a model of TFR2's function in murine erythropoiesis, indicating that deficiency in this receptor is associated with increased erythroid development and expression of EPO and ERFE in extrahepatic tissues independent of TFR's role in the liver.

Hereditary hemochromatosis (HH)[3] is a prevalent, autosomal recessive disease characterized by a disruption in iron regulation, resulting in systemic iron overload (1). Mutations in several genes can lead to HH, causing a wide variety of symptoms and severities. The more severe forms of HH result in cardiomyopathy, type 2 diabetes, arthritis, cirrhosis, and hepatocellular carcinoma (2, 3). Genetic studies have allowed HH to be divided into four subtypes according to the involved genes and affected pathways, with type 3 HH being characterized by the presence of one or more mutations in the gene encoding the single-pass type 2 membrane protein transferrin receptor 2 (*Tfr2*) (4).

Much like its homologue TFR1, TFR2 is capable of binding and internalizing iron-loaded transferrin (holo-Tf) (5). However, although TFR1 is expressed ubiquitously, TFR2 is largely restricted to hepatocytes and maturing erythrons (6), with liver having ~6-fold more TFR2 than TFR1 (7). Unlike *Tfr1*, liver-specific knockout of murine *Tfr2* results in iron overload (8, 9), implying that iron uptake is not the primary function of TFR2.

Significant differences also exist between *Tfr1* and *Tfr2* mRNA regulation. In contrast to *Tfr1*, *Tfr2* mRNA lacks the multiple iron-responsive elements contained within its 3′-UTR (5, 10). Consequently, the levels of *Tfr2* mRNA are independent of cellular iron. Interestingly, holo-Tf increases the stability of TFR2, but not TFR1, thereby increasing the amount of cellular TFR2 2–3-fold (11, 12). This stabilization occurs by inhibiting cleavage of TFR2 at the cell surface or by redirecting TFR2 from a late endosomal pathway to a recycling pathway (11–14). Given their unique expression patterns and regulation, the functions of TFR1 and TFR2 are likely to be different.

The first mutation implicating TFR2 in the regulation of iron homeostasis was a nonsense mutation in codon 250 (Y250X) (15). Subsequently, other HH-associated missense and nonsense mutations in the *TFR2*-coding region were identified (16). Mice homozygous for the orthologous nonsense mutation ($Tfr2^{Y245X/Y245X}$ or $Tfr2^{def}$) have undetectable levels of TFR2 protein and lowered levels of *Tfr2* mRNA in the liver (17). Iron homeostasis is heavily affected in $Tfr2^{def}$ mice, with increased iron uptake in the duodenum, elevated serum and liver iron, and decreased splenic iron (18). These mice also display abnormally low expression of hepcidin (*Hamp*), a hormone primarily

This work was supported by National Institutes of Health Grants R01-DK072166, R37-DK054488, R01DK109694, and R01DK102791, American Heart Association Grant 11POST5250029, and a Collins Medical Trust grant (to J. C.). The authors declare that they have no conflicts of interest with the contents of this article. The content is solely the responsibility of the authors and does not necessarily represent the official views of the National Institutes of Health.

This article contains Figs. S1–S5 and Tables S1–S3.

[1] Present address: Novus International Inc., St. Charles, MO 63304.

[2] To whom correspondence should be addressed: Dept. of Cell, Developmental and Cancer Biology, Oregon Health and Science University, L215, 3181 SW Sam Jackson Park Rd., Portland, OR 97239. Tel.: 503-4945845; E-mail: ennsca@ohsu.edu.

[3] The abbreviations used are: HH, hereditary hemochromatosis; BFU-E, burst-forming unit–erythroid; BM, bone marrow; CD, control diet; CFC, colony-forming cell; CFU-E, colony-forming unit–erythroid; EPO, erythropoietin; ERFE, erythroferrone; Hb, hemoglobin; Hct, hematocrit; HIF2α, hypoxia-inducible factor 2α; IDD, iron-deficient diet; MCH, mean corpuscular hemoglobin; MCV, mean corpuscular volume; ProE, proerythroblasts; RBC, red blood cell; RDW, red blood cell distribution width; SD, standard diet; Tf, transferrin; TFR1, transferrin receptor 1; TFR2, transferrin receptor 2; ANOVA, analysis of variance; HBSS, Hanks' balanced salt solution; PI, propidium iodide; rm, recombinant mouse; qRT-PCR, quantitative RT-PCR.

expressed in hepatocytes that is necessary for suppressing iron absorption in the small intestines (19).

Although *Tfr2* is also expressed in several erythroid progenitor populations (20), studies addressing the effect of TFR2 during erythropoiesis have reported contradictory findings. Lethally-irradiated wildtype (WT) mice that received bone marrow (BM) from $Tfr2^{-/-}$ mice had abnormal blood parameters, including elevated red blood cell (RBC) counts and hemoglobin (Hb) but reduced mean corpuscular volume (MCV) and mean corpuscular hemoglobin (MCH) (21). Conversely, a Cre-lox–generated BM-specific knockout of *Tfr2* showed no significant differences in the blood indices (22). The reported effect of TFR2 deficiency on erythropoietic populations in the BM and spleen also varies, with some studies showing a significant delay in maturation only when mice lacking TFR2 are maintained on an iron-deficient diet (IDD) (21–23). These dissimilar results warrant new approaches to reveal the function of TFR2 during erythropoiesis.

Our initial analysis of $Tfr2^{def}$ mice revealed changes to circulating RBCs and the total cell population of the BM and spleen independent of iron overload. From these findings, we hypothesized that examination of the BM and splenic erythroid populations in $Tfr2^{def}$ mice would also reveal iron overload-independent changes. To do so, we utilized a robust staining panel that was developed by Chen *et al.* (24, 25) and further refined by Doty *et al.* (26) to accurately capture the physiological progression of erythroid development in murine BM and spleen. Erythroid maturation takes place in two phases: erythroid progenitor proliferation and then terminal erythroid development. Progenitor proliferation begins when hematopoietic stem cells differentiate into burst-forming unit–erythroid (BFU-E), which in turn differentiate into colony-forming unit–erythroid (CFU-E) (27). Terminal erythroid differentiation begins with the formation of proerythroblasts (ProE) from CFU-E, which then undergo three mitoses to form basophilic, polychromatic, and then orthochromatic erythroblasts. Each phase can be identified by cell size, chromatin condensation, hemoglobinization, and the abundance of the cell-surface markers Ter119 and CD44 (28).

Cytometric analysis of BM erythroid populations from $Tfr2^{def}$ mice revealed decreased BFU-E, CFU-E, and ProE populations and increased orthochromatic erythroblasts, whereas the spleens of $Tfr2^{def}$ mice had an increase in both erythroid progenitor proliferation and terminal differentiation. Importantly, these changes in the BM and spleen persisted in the absence of iron overload and when liver TFR2 expression was restored in $Tfr2^{def}$ mice. TFR2-deficient mice also had an iron load independent increase in the expression of the hormone erythroferrone (*Erfe*) and an increase in the serum of the erythropoietic hormone, erythropoietin (EPO). Taken together, our findings describe a new regulation of EPO by extrahepatic TFR2 that is not reliant on anemia or hypoxia.

Results

$Tfr2^{def}$ mice have enlarged spleens in the absence of iron overload

WT and $Tfr2^{def}$ mice were maintained on a control or iron-deficient diet (CD or IDD, respectively) for 6 – 8 weeks, starting at 4 weeks of age in order to identify the iron-overload independent effects of *Tfr2* deficiency on erythropoiesis. Initial observations revealed a diet independent increase in relative spleen mass of $Tfr2^{def}$ mice when compared with WT mice (Fig. 1*A*). Furthermore, the enlargement of $Tfr2^{def}$ spleens correlated with a 30% increase in nucleated splenic cells regardless of diet (Fig. 1*B*), which indicated that the increased size of the spleen was not due to edema. Interestingly, the number of nucleated cells in the femur of $Tfr2^{def}$ mice on CD decreased by 11% (Fig. 1*C*), a finding consistent with a recent report that revealed an increase in bone mineral density, and an accompanying decrease in bone marrow volume for $Tfr2^{def}$ mice (29).

$Tfr2^{def}$ mice maintained on CD also displayed the well-characterized increase in nonheme liver iron, serum iron concentration, and Tf-saturation, with a decrease in nonheme splenic iron (Fig. 1, *D–G*). When maintained on IDD, nonheme liver iron normalized in $Tfr2^{def}$ mice (Fig. 1*D*), whereas nonheme splenic iron remained low (Fig. 1*G*). Serum iron and Tf saturation remained elevated in $Tfr2^{def}$ mice maintained on IDD (Fig. 1, *E* and *F*), indicating a continued release of iron stores into the blood.

Interestingly, $Tfr2^{def}$ mice displayed a decrease in nonheme kidney iron that was independent of dietary iron (Fig. 1*H*). Iron is an important regulator of EPO, a hormone produced in the interstitial fibroblasts of the kidney (30, 31). Phlebotomy-induced anemia elevates *Epo* mRNA, which can be alleviated with intraperitoneal iron administration (32). Thus, the decrease in kidney iron in $Tfr2^{def}$ mice may be associated with higher serum EPO. Consistent with this hypothesis, serum EPO levels were increased by 50 and 60% in $Tfr2^{def}$ mice on CD or IDD, respectively (Fig. 1*I*). The iron-overload independent effect of TFR2 deficiency on serum EPO combined with the changes to the total cell population of the BM and spleen indicate a direct role for TFR2 in hematopoiesis and EPO regulation.

$Tfr2^{def}$ mice exhibit a mild anisocytosis independent of iron load

When compared with WT mice, $Tfr2^{def}$ mice displayed a mild microcytic anemia, as evidenced by a decrease in the number of circulating RBCs, Hb, hematocrit (Hct), and MCV, and an increase in the RBC distribution width (RDW) (Table 1). Maintaining $Tfr2^{def}$ mice on IDD normalized RBC count, Hb, and Hct, but it had no noticeable effect on MCV, MCH, and RDW, with $Tfr2^{def}$ mice sustaining a 7% increase in RDW independent of iron overload. RDW is a measurement of the heterogeneity of distribution of red blood cell size (33) and has classically been used in combination with MCV to diagnose anemias in patients (34). A high RDW, also known as anisocytosis, is often the result of abnormal or incomplete erythropoiesis (35). In TFR2-deficient mice, the presence of an elevated RDW in the absence of both iron overload and mild anemia further highlights the effect TFR2 has on erythropoiesis and suggests that the loss of TFR2 has a significant negative effect on terminal erythroid development.

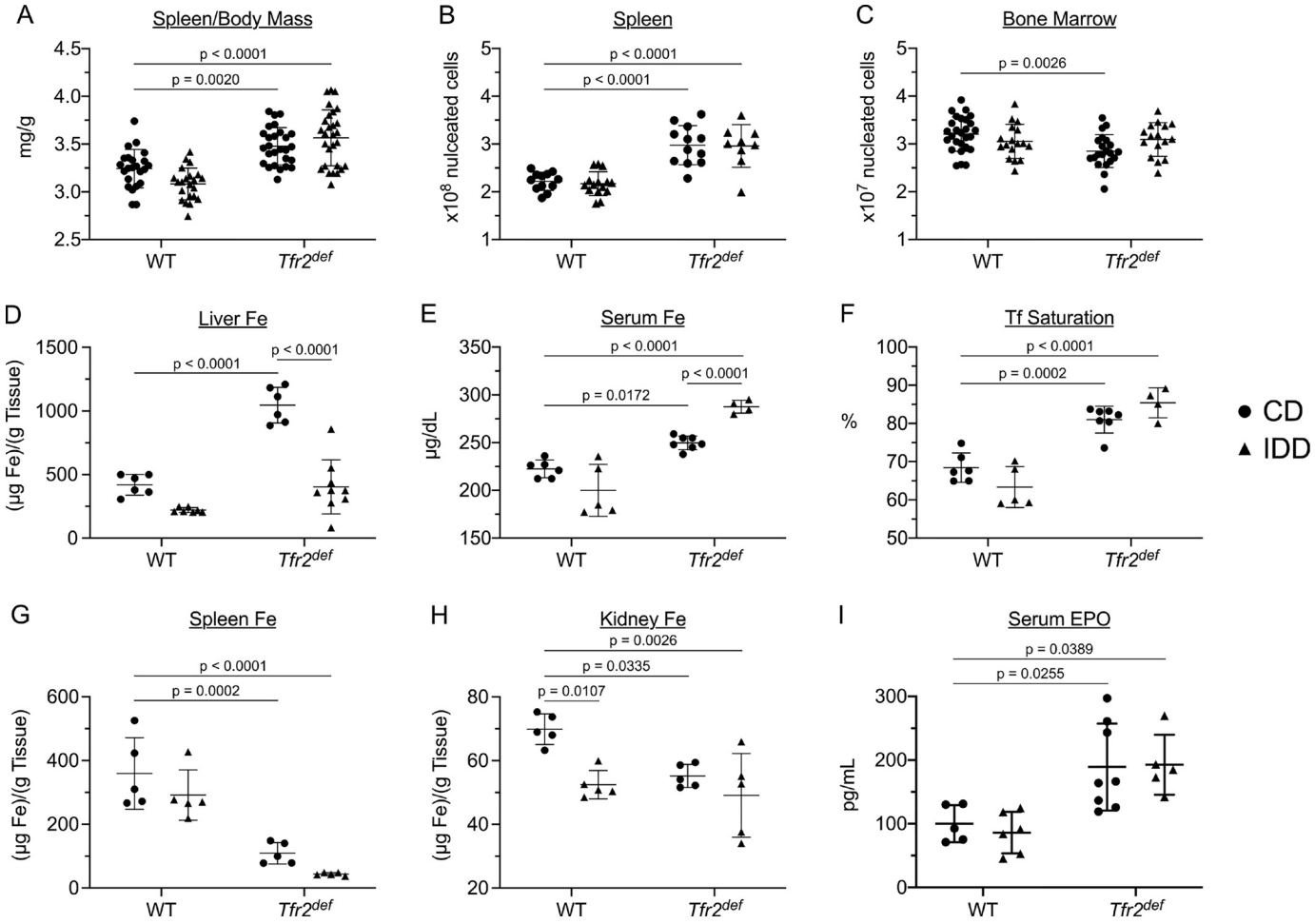

Figure 1. TFR2 deficiency is associated with increased spleen mass and decreased spleen and kidney iron independent of iron overload. *A,* spleen mass per body mass. *B,* total nucleated cells in the spleen. *C,* total nucleated bone marrow cells in the femur. *D,* liver nonheme iron (wet tissue). *E,* serum iron concentration. *F,* serum transferrin saturation. *G,* spleen nonheme iron (wet tissue). *H,* kidney nonheme iron (wet tissue). *I,* serum EPO concentrations for WT and *Tfr2*^{def} mice on CD or IDD measured via ELISA. Statistics were calculated using Tukey's multiple comparisons test following two-way ANOVA.

Table 1

RBC distribution width is increased in *Tfr2*^{def} mice independent of iron overload

RBC, red blood cells; Hb, hemoglobin; HCT, hematocrit; MCH, mean corpuscular hemoglobin; MCHC, mean corpuscular hemoglobin concentration; Retics, reticulocytes. $n = 10–16$. Statistics were calculated using Tukey's multiple comparisons test following two-way ANOVA.

	WT on CD	WT on IDD	*Tfr2*^{def} on CD	*Tfr2*^{def} on IDD
RBC (M/µl)	8.09 ± 0.28	7.88 ± 0.20	7.77 ± 0.23 ($p = 0.0143$)[a]	8.24 ± 0.35 ($p = 0.0001$)[b]
Hb (g/dl)	11.7 ± 0.3	11.4 ± 0.4	11.3 ± 0.5 ($p = 0.0009$)[a]	11.6 ± 0.5 ($p = 0.0180$)[b]
Hct (%)	46.2 ± 2.0	43.6 ± 1.6 ($p = 0.0163$)[a]	43.4 ± 1.2 ($p = 0.0001$)[a]	45.7 ± 1.9 ($p = 0.0020$)[b]
MCV (fl)	57.1 ± 1.5	55.3 ± 1.2 ($p = 0.0129$)[a]	55.9 ± 1.1	55.5 ± 2.0 ($p = 0.0277$)[a]
MCH (pg)	14.5 ± 0.3	14.5 ± 0.4	14.4 ± 0.4	14.1 ± 0.5 ($p = 0.0269$)[a]
MCHC (g/dl)	25.5 ± 0.8	26.1 ± 0.6	25.7 ± 0.6	25.4 ± 0.5
RDW (%)	17.7 ± 0.6	17.9 ± 0.3	19.0 ± 0.6 ($p < 0.0001$)[a]	19.0 ± 0.5 ($p < 0.0001$)[a]
Retics (%)	5.34 ± 1.22	5.13 ± 0.65	6.41 ± 1.82	5.16 ± 0.72

[a] Data were compared with WT on CD.
[b] Data were compared with *Tfr2*^{def} on CD.

Splenic CFU-E frequency increases in Tfr2^{def} *mice independent of iron overload*

The observed anisocytosis and increased serum EPO levels lead us to further investigate the iron-independent effects of TFR2 deficiency on the identifiable stages of erythropoiesis. To do so, we employed the use of an *in vitro* hematopoietic colony-forming cell (CFC) assay to quantify the first two stages of erythropoiesis: BFU-E and CFU-E (Fig. 2).

In mice, exogenously elevating systemic EPO levels will bias hematopoietic stem and progenitor cells to undergo erythropoiesis (36). Moreover, the proliferation and differentiation of CFU-E cells is entirely dependent on the presence of EPO (30). When assayed in the presence of EPO and other key hematopoietic cytokines, the bone marrow of *Tfr2*^{def} mice produced ~20% fewer BFU-E colonies than WT, whereas splenic BFU-E frequency was similar to WT regardless of TFR2 and iron status (Fig. 2, *A* and *B*). Conversely, the frequency of CFU-E colonies formed from BM tissue was similar across all groups, whereas the *Tfr2*^{def} spleens revealed an increase in CFU-E progenitors regardless of iron status (Fig. 2, *C* and *D*). These results suggest

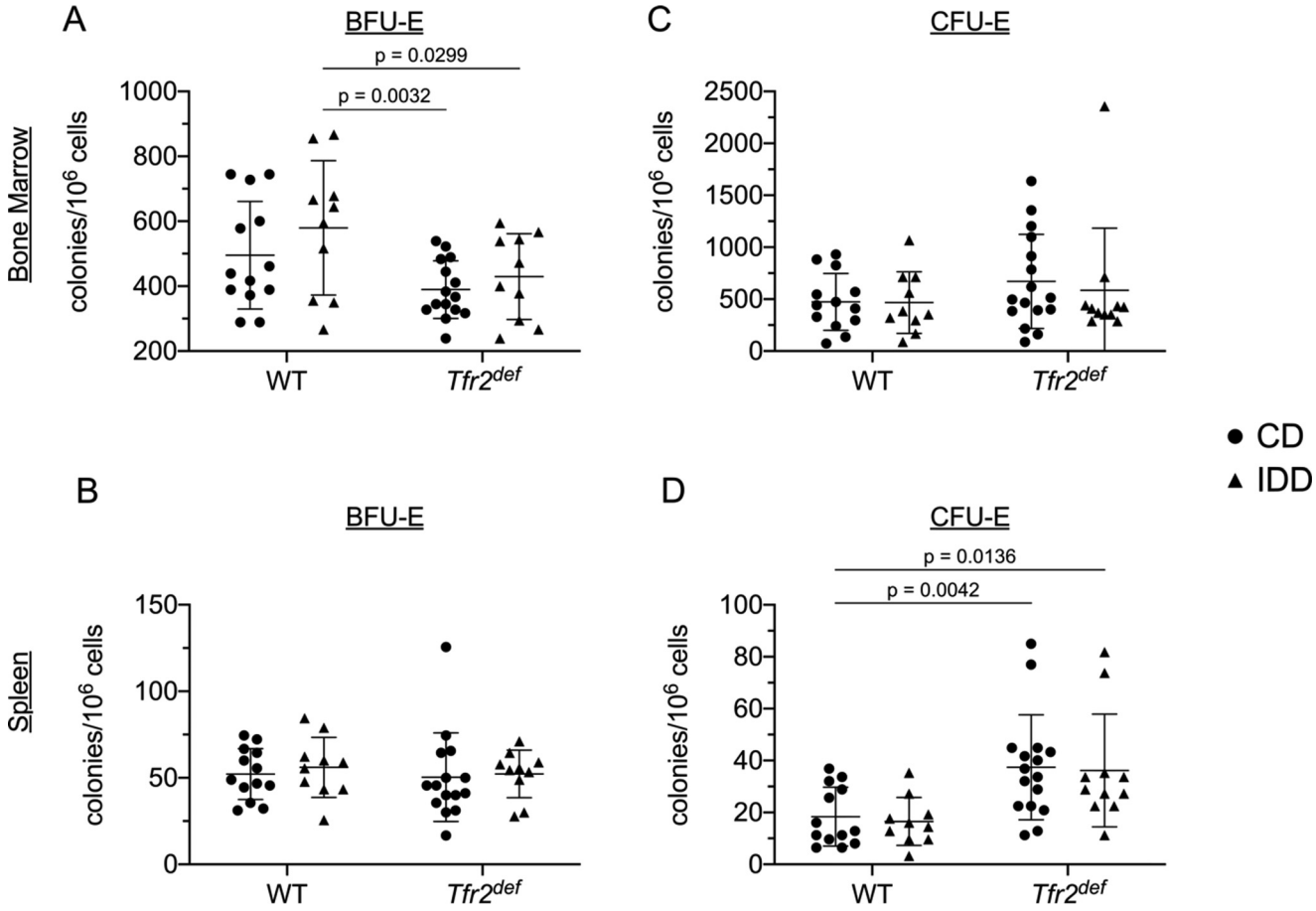

Figure 2. Serum EPO and splenic CFU-E progenitor cells are elevated in *Tfr2*^{def} mice independent of iron overload. *A–D,* single cell suspensions from BM and spleen were plated using methylcellulose media. Colonies formed from BM BFU-E (*A*), spleen BFU-E (*B*), BM CFU-E (*C*), and spleen CFU-E (*D*) progenitors were quantified 2 days (for CFU-E colonies) and 10 days (for BFU-E colonies) after plating. Data are shown as number of colonies that formed per 10^6 nucleated cells. Statistics were calculated using Fisher's LSD test following two-way ANOVA.

that TFR2 deficiency leads to a loss of the early erythroid progenitors in the bone marrow and an expansion of the developing erythroid compartment in the spleen.

TFR2 deficiency increases erythroblast frequency

To quantify the later stages of erythropoiesis, we employed a flow cytometry staining protocol developed by Chen *et al.* (24) and Liu *et al.* (25) and further modified by Doty *et al.* (26) that utilizes Ter119, CD71, CD44, and size to distinguish discrete stages of erythroid maturation from erythroid progenitors to RBCs (see Fig. S1 for gating technique). Specifically, this protocol allows for the identification and isolation of five populations from the BM and spleen: population I, BFU-E, CFU-E, and proE; population II, basophilic erythroblasts; population III, polychromatic erythroblasts; population IV, orthochromatic erythroblasts; and population V, reticulocytes and RBCs.

Analysis of populations I–IV in the femoral BM of WT mice verified the staining procedure, yielding a ratio of 1.0:2.5:3.3:9.2, close to the predicted 1:2:4:8 (Fig. 3, *A–F*) (25). In the BM of *Tfr2*^{def} mice maintained on CD or IDD, population I was decreased by 25 and 20%, respectively, when compared with the control group (Fig. 3*C*). These results agree with the results in Fig. 2*A*, which showed a loss in the BFU-E population of *Tfr2*^{def} BM. Additionally, we detected an iron-overload independent increase in the BM orthochromatic erythroblasts (population IV) for *Tfr2*^{def} mice (21% when fed CD and 28% when fed IDD, Fig. 3*F*).

The spleens of *Tfr2*^{def} mice displayed a more pronounced phenotype. Populations I–IV were elevated by ~2-, 6-, 6-, and 3-fold in the spleen from *Tfr2*^{def} mice regardless of iron load (Fig. 3, *G–L*). The iron-overload independent increase in population I is consistent with the results obtained using the CFC assay, where a large increase in splenic CFU-E frequency of *Tfr2*^{def} mice was observed with or without iron overload (Fig. 2*D*).

One explanation for the loss of early erythroid progenitors and the increase in late-stage erythropoiesis in the BM of *Tfr2*^{def} mice would be that *Tfr2*^{def} mice have exceeded the self-renewal and differentiation capacity for erythropoiesis in the femur, which is then compensated for by an increase in erythropoiesis in the spleen. Furthermore, the continuation of these changes in the absence of iron overload highlights the direct role of TFR2 signaling throughout erythropoiesis.

Hepatic-specific restoration of TFR2 normalizes kidney iron, spleen iron, and spleen mass

To further investigate the possibility that TFR2 deficiency in the liver may affect erythropoiesis, *Tfr2*^{def} mice were injected

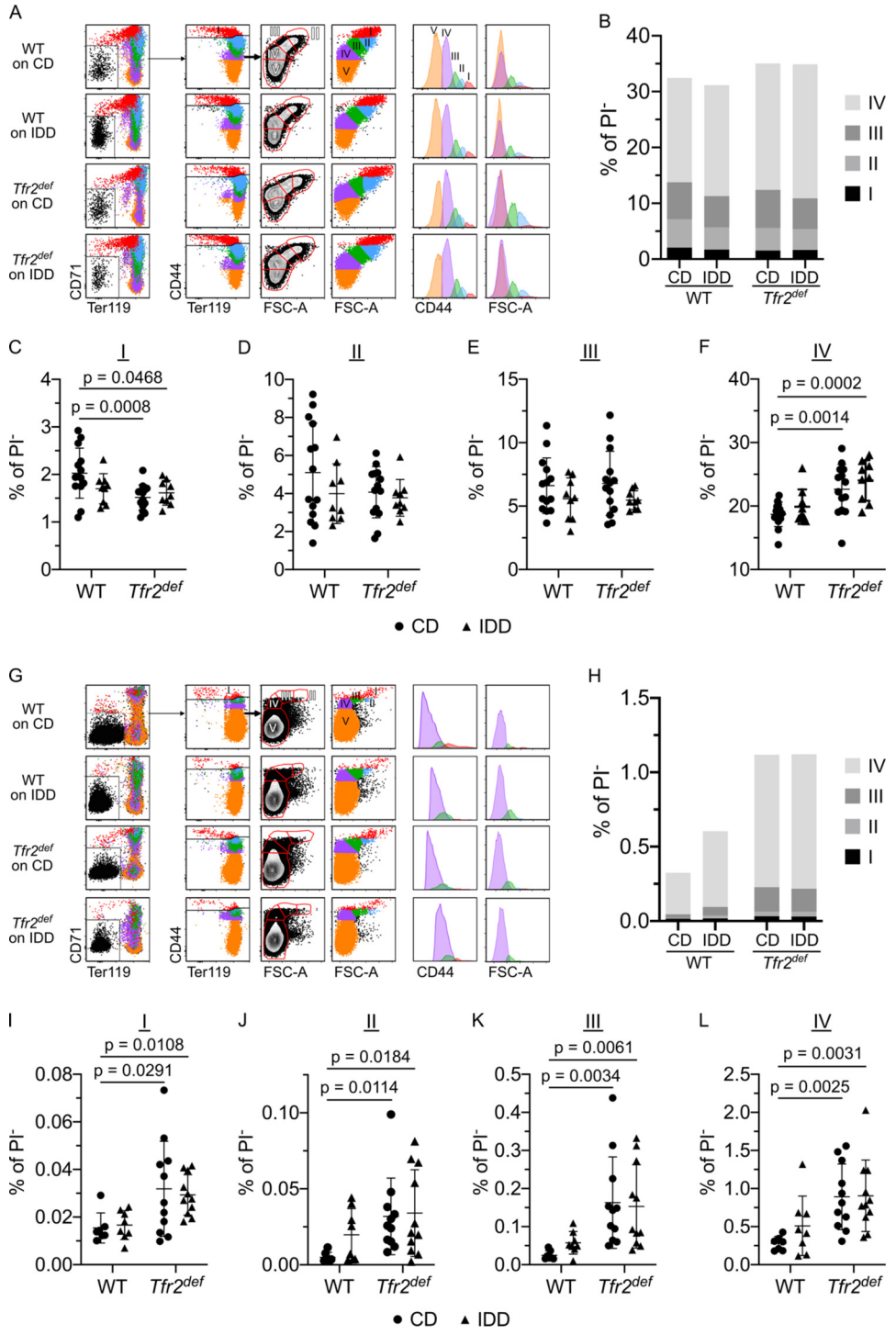

Figure 3. Bone marrow and splenic erythroblasts are elevated in *Tfr2*^{def} mice independent of iron overload. Hematopoietic progenitor cells isolated from femoral BM (*A–F*) and spleen (*G–L*) were stained and analyzed via flow cytometry. *A* and *G*, representative flow plots from isolated marrow and splenic cells of WT or *Tfr2*^{def} mice on either CD or IDD. Committed erythroid cells were identified by the removal of CD71^{low}Terr119^{low} cells after the removal of lineage negative (B220^{-}Gr1^{-}CD11b^{-}, or lin^{-}) cells. The resulting population was then gated using CD44, Ter119, and forward scatter (FSC) so as to identify the following populations: (*I*) BFU-E/CFU-E/ProE erythroblasts (*red*); (*II*) basophilic erythroblasts (*blue*); (*III*) polychromatic erythroblasts (*green*); (*IV*) orthochromatic erythroblasts (*purple*); and (*V*) reticulocytes and RBC (*orange*). Data are shown as dot or 2% contour plots. Histograms of CD44 and FSC are shown for size and distribution comparison. Total frequency of populations *I–IV* shown are a percentage of live (PI^{-}) cells in either the femoral BM (*B*) or spleen (*H*). Frequency of individual erythroid populations were quantified in the femoral BM (*C–F*) and spleen (*I–J*). Statistics were calculated using Fisher's LSD test following two-way ANOVA.

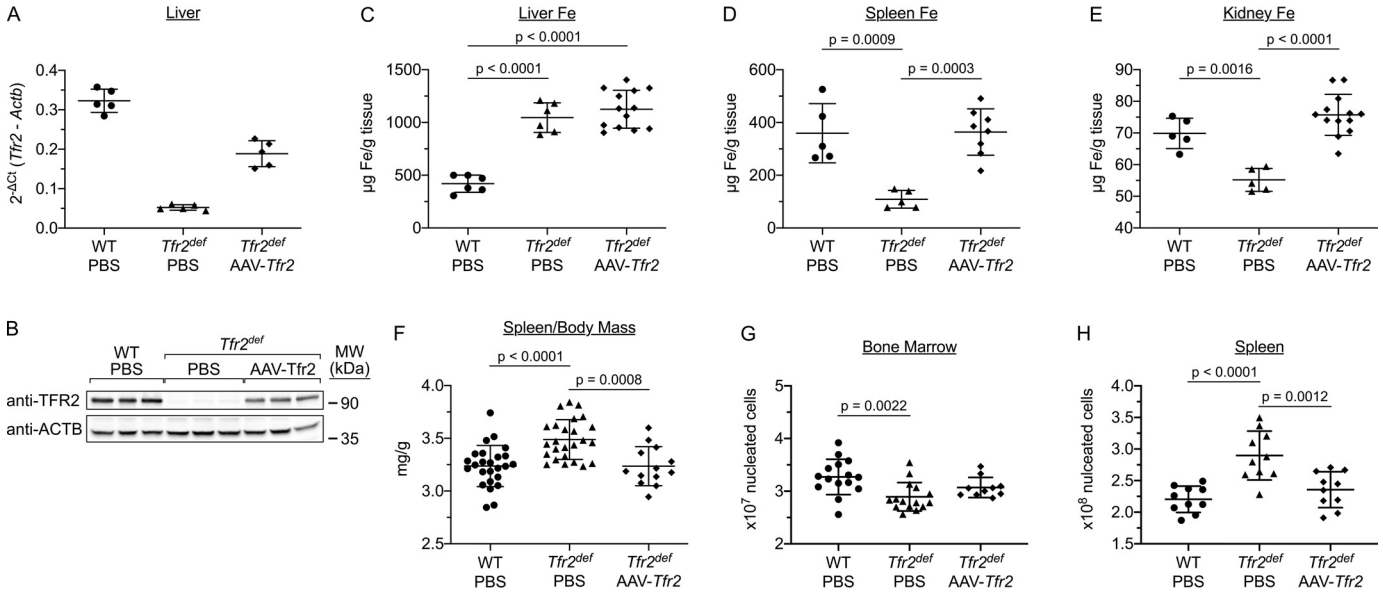

Figure 4. Hepatocyte-specific restoration of TFR2 normalizes spleen Fe, kidney Fe, and total hematopoietic cell count. Eight-week-old WT and *Tfr2*^{def} mice on CD received i.v. injections of either PBS alone or PBS containing 1.6×10^{12} vg (virus genomes) of AAV2/8-*Tfr2*. Tissue was collected 3 weeks later. *A*, liver *Tfr2* mRNA expression, relative to β-actin (*Actb*) mRNA. *B*, immunoblot on whole-liver extract using anti-TFR2 and anti-ACTB antibodies. Nonheme iron (using wet tissue) in the liver (*C*), spleen (*D*), and kidney (*E*). *F*, ratio of spleen to body mass; *G*, total nucleated cell count of the femur; and *H*, total nucleated cell count of the spleen. Statistics were calculated using Fisher's LSD test following one-way ANOVA.

via tail vein with an AAV2/8 virus encoding the full-length murine *Tfr2* ORF under the regulation of a hepatocyte-specific promoter (AAV2/8-*Tfr2*). PBS-injected mice were used as controls because previously published PBS- and AAV2/8-GFP–injected mice indicated no differences in responses to any of the parameters measured (37, 38). RT-quantitative PCR and Western blot analysis confirmed liver-specific expression of TFR2 3 weeks after injection (Fig. 4, *A* and *B*, and Fig. S2, *A–D*). *Hamp* and *Id1* mRNAs were also restored to WT levels, whereas the IL6 levels remained low, indicating that the increase in *Hamp* and *Id1* was not due to an inflammatory response, which also induces hepcidin production (Fig. S2, *D–F*).

Even though *Hamp* and *Id1* mRNA returned to that of WT mice, nonheme liver iron and serum iron did not change 3 weeks after expression of hepatic TFR2 in *Tfr2*^{def} mice (Fig. 4*C* and Fig. S2*G*). Blood analysis revealed that *Tfr2*^{def} mice expressing hepatic TFR2 had an increase in Hb but maintained an elevated RDW and a low RBC count (Table S1). Conversely, nonheme iron in the spleen and kidney increased to levels observed in WT mice (Fig. 4, *D* and *E*). Interestingly, a normalization of spleen mass was also observed in *Tfr2*^{def} mice injected with AAV–*Tfr2*, suggesting a possible role for hepatic TFR2 in hematopoiesis (Fig. 4*F*). Likewise, the total cell count of the femur and spleen in *Tfr2*^{def} mice injected with AAV–*Tfr2* normalized to WT levels (Fig. 4, *G* and *H*). These changes to kidney iron and the hematopoietic compartments reveal a possible regulatory effect of hepatic TFR2 on EPO expression and hematopoiesis. Therefore, serum EPO and the erythroid populations in *Tfr2*^{def} mice expressing hepatic TFR2 were analyzed to determine whether erythropoiesis is significantly affected by hepatic TFR2.

Hepatocyte-specific restoration of TFR2 does not affect erythropoiesis

Remarkably, EPO levels in the blood remained elevated 3 weeks after injecting *Tfr2*^{def} mice with AAV–*Tfr2* even after normalization of kidney iron (Fig. 5*A*). Additionally, cytometric analysis revealed that expression of TFR2 in hepatocytes of *Tfr2*^{def} mice did not affect the percentage of erythroid progenitor cells in either the bone marrow or spleen (Fig. 5, *B–K*), even though the total amount of femoral and splenic cells normalized (Fig. 4, *G* and *H*). The BM of *Tfr2*^{def} mice injected with AAV–*Tfr2* maintained a decrease in population I and an increase in population IV (Fig. 5*D*), whereas all three populations of erythroblasts (populations II–IV) remained elevated in the spleen (Fig. 5, *I–K*). These findings support the hypothesis that the expression and function of TFR2 outside of the liver are critical for the regulation of erythropoiesis.

TFR2 deficiency increases Erfe expression in bone marrow polychromatic erythroblasts independent of iron overload

During erythropoiesis, expression of the hormone erythroferrone (*Erfe*) is initiated in proE cells, and peaks in polychromatic erythroblast (39). Moreover, its expression can be induced via phlebotomy (40) or intravenous administration of EPO (41). ERFE acts to suppress *Hamp* expression in the liver. As a result, *Erfe*$^{-/-}$ mice have elevated levels of serum hepcidin and a delayed normalization of serum iron level after the induction of anemia (40). Given the increase in erythroid precursor cells and serum EPO in *Tfr2*^{def} mice, we hypothesized that *Erfe* expression would also be elevated.

Analysis of *Erfe* expression in BM erythroid populations isolated from WT and *Tfr2*^{def} mice on either CD or IDD showed a 2-fold or greater increase in populations I–III in *Tfr2*^{def} mice with or without iron overload (Fig. 6, *A–C*). Although *Erfe*

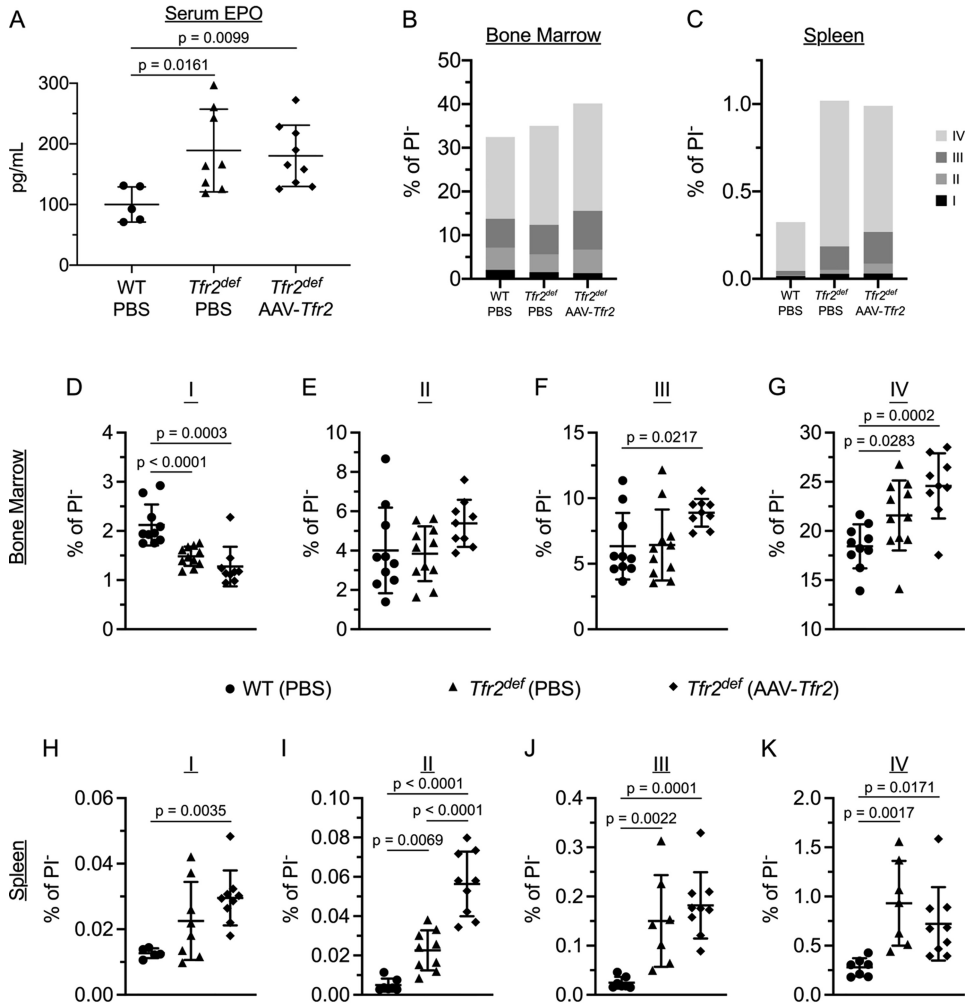

Figure 5. Hepatocyte-specific restoration of Tfr2 does not normalize erythroblast frequency in bone marrow and spleen. Eight-week-old mice on CD were injected with PBS or AAV2/8-*Tfr2*. Three weeks later, BM cells, splenic cells, and serum were collected and analyzed. *A,* serum EPO concentration was quantified using ELISA. Frequency of erythroid populations in the femur (*B* and *D–G*) and spleen (*C* and *H–K*) is represented as a percentage of live (PI^-) cells: *D* and *H,* BFU-E, CFU-E, and ProE (*population I*); *E* and *I,* basophilic erythroblasts (*population II*); *F* and *J,* polychromatic erythroblasts (*population III*); *G* and *K,* orthochromatic erythroblasts (*population IV*). Statistics were calculated using Fisher's LSD test following one-way ANOVA.

mRNA was reliably amplified in *Tfr2*^{def} basophilic erythroblasts of the spleen (Fig. S3*C*), expression of *Erfe* was undetectable in equivalent WT populations even though the C_t for the reference gene (*Gapdh*) was consistent across within all populations (Fig. S3*D*). These results support the observed increase in erythroid lineage cells in the BM and spleen of *Tfr2*^{def} mice and emphasize an important role for TFR2 in suppressing the production of EPO and ERFE.

Discussion

The data presented here highlight the significant effect TFR2 has on the regulation of erythropoiesis. The initial observation of enlarged spleens, reduced BM cells, and increased nucleated splenic cells in *Tfr2*^{def} mice signified a heavier reliance on extramedullary hematopoiesis, and the discovery of TFR2 deficiency-associated anisocytosis in the absence of iron overload further emphasizes the role of TFR2 during erythropoiesis. Through the utilization of a retrospective colony assay and flow cytometry, TFR2-deficient BM was found to be associated with a decrease in the earliest erythroid progenitor, BFU-E, and an increase in the last stage before enucleation (orthochromatic erythroblasts). The spleens of *Tfr2*^{def} mice had a more pronounced increase in erythropoiesis, with an expansion of CFU-E and all three erythroblast populations. These changes agree with the elevated serum EPO and in *Erfe* expression levels (Fig. 6*D*).

Prior publications have also investigated how TFR2 deficiency affects RBC maturation, often with conflicting results (17, 21–23, 42–44). The initial characterization of *Tfr2*^{def} mice found no abnormalities in the circulating blood (17). A later report showed increased RDW in *Tfr2*^{def} mice compared with WT mice when on a mixed C57BL6/J-FVB/J background (45). Furthermore, analyses of adult *Tfr2*$^{-/-}$ mice on a 129/sv background revealed increases in Hb and MCH or increases in Hb and Hct (42, 43). In this report, we found decreases in circulating RBCs, Hb, and Hct in iron-overloaded *Tfr2*^{def} mice on an FVB background that normalized when *Tfr2*^{def} mice were maintained on a low-iron diet. In addition, we found a decrease in MCV and an elevated RDW in *Tfr2*^{def} mice regardless of iron overload. Some of these differences may be due to the use of dissimilar breeds of mice. Strain differences can affect iron

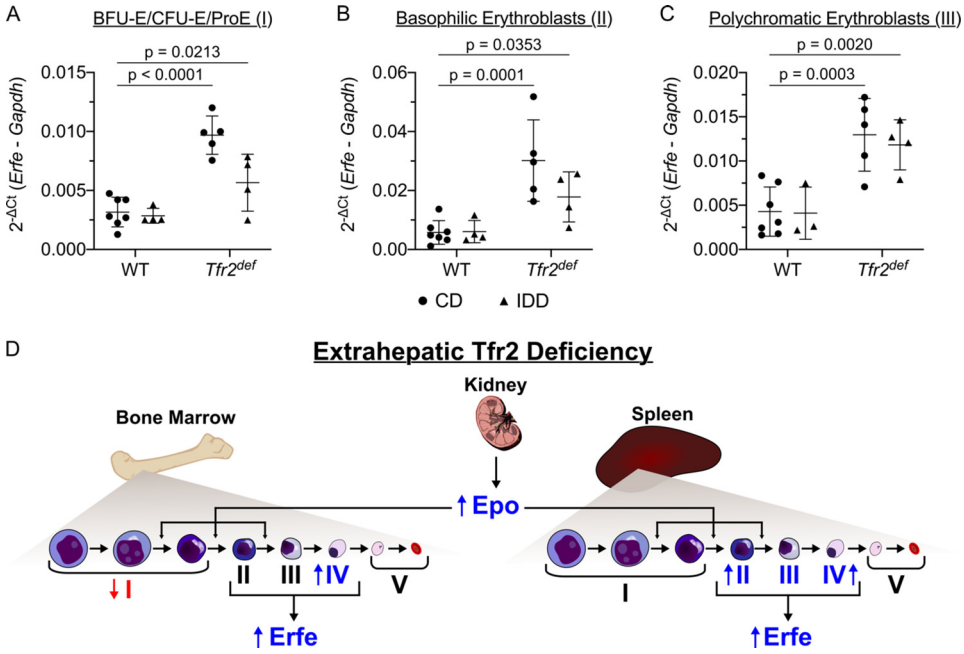

Figure 6. TFR2 deficiency increases *Erfe* expression in bone marrow polychromatic erythroblasts independent of iron overload. Femoral BM cells from WT and *Tfr2*^{def} mice maintained on CD or IDD were sorted as in Fig. 3. Expression of *Erfe* mRNA, relative to *Gapdh* mRNA, was quantified using qRT-PCR for the following: *A,* population I (BFU-E, CFU-E, and ProE); *B,* population II (basophilic erythroblasts); and *C,* population III (polychromatic erythroblasts). Statistics were calculated using Fisher's LSD test following two-way ANOVA. *D,* extrahepatic TFR2 regulates EPO, *Erfe,* and erythropoiesis independent of iron load. Higher levels of serum Epo in *Tfr2*^{def} mice are associated with a loss of early erythroid progenitors and an increase in orthochromatic erythroblasts in the bone marrow. The frequency of erythroblasts in the spleens of *Tfr2*^{def} mice is increased at all three stages. The increase in erythroid differentiation in the BM and spleen is accompanied by a modest increase in *Erfe* expression, which is insufficient to suppress the induction of *Hamp* expression by hepatic TFR2. *I,* BFU-E, CFU-E, and proE; *II,* basophilic erythroblasts; *III,* polychromatic erythroblasts; *IV,* orthochromatic erythroblasts; and *V,* reticulocytes and RBCs.

loading and *Hamp* expression (46, 47). Nevertheless, the findings presented here demonstrate that the anisocytosis associated with TFR2 deficiency is not a secondary effect caused by iron overload, but originates from a more direct loss of regulation imposed by TFR2.

Previously, hematopoietic progenitor cells isolated from the BM of *Tfr2*$^{-/-}$ mice were reported to have a decrease in CFU-E colonies when grown in media supplemented with EPO alone (23). Here, no changes in BM CFU-E were observed when colonies were established using media supplemented with EPO and the cytokines SCF, IL-3, and IL-6. Both IL-3 and SCF can affect CFU-E cell maturation *in vitro* (48, 49). Hence, the presence or absence of these cytokines may influence changes to erythropoiesis caused by a lack of TFR2, which would account for the observed differences in erythroid progenitors between studies.

Much like the analysis of RBCs and early erythroid progenitors, varying differences in terminal erythroid differentiation have been described for mice lacking TFR2 (21–23). Forejtnikovà *et al.* (23) observed a delay in both maturation and hemoglobinization when *TFR2* was knocked down in human erythroid progenitor cells *in vitro*. When BM-specific *Tfr2* knockout mice (*Tfr2*^{BMKO}) were generated by transplanting lethally-irradiated WT mice with BM from *Tfr2*$^{-/-}$ mice, Nai *et al.* (21) observed an increase in basophilic and polychromatic erythroblast populations when *Tfr2*^{BMKO} mice were maintained on an iron-balanced diet but not while on an IDD. Conversely, BM-specific *Tfr2* knockout mice generated using the *Vav-Cre* allele had an accumulation of immature erythroid cells only when maintained on an iron-deficient diet (22).

To accurately delineate the effects of TFR2 on erythropoiesis, a method that correctly quantifies the population of erythroid cells at each discrete stage of differentiation is critical. Consequently, we used a protocol that allows for the removal of all populations of cells that stain positive for lymphocyte, granulocyte, and monocyte lineage and stain negative for CD71 and Ter119. Similar to Doty *et al.* (26), we included CD71^{high}Ter119^{low} cells in our early erythroid population (population I) so as to include BFU-E and CFU-E cells (50, 51).

Using this method, the observed frequencies of BM erythroid populations in the control group were consistent with the model established by Liu *et al.* (25). By comparison, femurs of *Tfr2*^{def} mice had a decrease in population I (BFU-E, CFU-E, and ProE) and an increase in population IV (orthochromatic erythroblasts), independent of iron overload. In the spleen of *Tfr2*^{def} mice, all three erythroblast populations were expanded regardless of diet. These results are in agreement with the data acquired from the hematopoietic CFC assay, where an absence of TFR2 was associated with an expansion of splenic CFU-E and a reduction in femoral BFU-E. The loss of early erythroid progenitors in *Tfr2*^{def} BM is also in accordance with the overall reduction in BM cells, which in turn agrees with the previously reported increase in bone mineral density of *Tfr2*^{def} mice (29).

Although expression of TFR2 in the hepatocytes of *Tfr2*^{def} mice did not significantly affect liver iron, serum iron, nor the frequency of erythroid progenitor populations, it did normalize nonheme iron in the kidney and spleen as well as the total amount of nucleated cells in the BM and spleen. These changes to the hematopoietic compartments of *Tfr2*^{def} mice injected with AAV–*Tfr2* may result from liver TFR2 affecting non-

erythroid lineages. Indeed, compared with PBS-injected *Tfr2*^{def} mice, there was a measurable decrease in the percentage of cells that stained positive for lymphocyte, monocyte/macrophage, and granulocyte lineage markers (lin$^+$ cells) in the BM of *Tfr2*^{def} mice injected with AAV–*Tfr2* (Fig. S4). Although it remains unknown exactly which nonerythroid lineages of the BM and spleen are affected by hepatic expression of TFR2, these data do reveal several new and interesting lines of inquiry.

The increase in erythroblast frequencies coincided with an iron-overload independent increase in *Erfe* expression in the polychromatic erythroblasts of *Tfr2*^{def} BM. ERFE has only recently been characterized as a regulator of iron metabolism (39). During anemia, or after treatment with EPO, *Erfe* expression increases, leading to hepcidin suppression and increased iron absorption (40, 41). The effect of TFR2 on *Erfe* expression has been previously studied in the spleen of transplant and conditional knockout models. *Tfr2*^{BMKO} mice generated by Nai *et al.* (21) showed an iron-overload independent increase in splenic *Erfe* mRNA, whereas *Tfr2*$^{\Delta/f}$/*Vav-Cre*$^{+/-}$ mice had *Erfe* expression increased in a splenic cell population containing mostly polychromatic erythroblasts (22). The results shown here reveal a regulatory role for TFR2 on *Erfe* expression in the BM, further confirming the importance of TFR2 on repressing erythropoiesis.

Particularly intriguing is the increase in serum EPO levels in *Tfr2*^{def} mice in the absence of hypoxia and iron deprivation. *Epo* expression in the interstitial fibroblasts of the kidney is positively regulated by the binding of hypoxia-inducible factor 2α (HIF2α) at a 5′-hypoxic response element in the *Epo* gene (52, 53). Upstream, *HIF2α* mRNA can be post-transcriptionally regulated at a 5′-iron–response element through the binding of iron-regulatory protein 1 (IRP1) (54). Mice lacking *Irp1* have elevated HIF2α in the kidney and EPO in the serum, as well as decreased nonheme iron in the kidney and liver (55, 56). Our data show that, even after restoration of TFR2 in the liver and normalization of iron in the kidney, EPO remains elevated in the serum (Fig. 4). This suggests another level of regulation for *Epo* expression that may be independent of the oxygen and iron status in the kidney. An earlier study reported low expression of *Tfr2* mRNA in the murine kidneys (10). Additional studies involving the effect of transferrin and its receptors in the kidney may yield new and interesting avenues for the regulation of iron homeostasis.

The results of these studies lead us to propose a model for the role of nonhepatic TFR2 in the regulation of erythropoiesis (Fig. 6*D*). Increased EPO levels in *Tfr2*^{def} mice lead to increased BFU-E and erythroid precursor cells. However, the modest increase of *Erfe* (Fig. 6, *A–C*) was not sufficient to prevent hepatic TFR2 from inducing *Hamp* expression when *Tfr2*^{def} mice were injected with AAV–*Tfr2* (Fig. S2*D*). Thus, hepatic and nonhepatic TFR2s act independently to regulate erythropoiesis. The question remains as to how the lack of nonhepatic TFR2 results in elevated EPO levels. We hypothesize that an absence of TFR2 in nonhepatic compartments leads to the synthesis of a hormone, possibly ERFE, which affects EPO production in the kidney. Alternatively, the EPO-producing cells in the kidney sense Tf saturation directly through the TFR2 receptor. An earlier report indicated a low level of *Tfr2* expression of *Tfr2* mRNA in the murine kidneys (10). Future studies will concentrate on distinguishing between these possibilities.

Experimental procedures

Animal husbandry and mouse models

Mice were bred and maintained in the animal house facilities of the Department of Comparative Medicine, Oregon Health and Science University, Portland, OR. Water and food were given *ad libitum*. All experimental protocols present were approved by the Institutional Animal Care and Use Committee at Oregon Health and Science University.

The previously described TFR2-deficient mouse model (17) was obtained from Dr. Robert E. Fleming (Saint Louis University) on the FVB/NJ strain (The Jackson Laboratory). *Tfr2*^{def} and WT FVB/NJ were maintained as separate colonies and interbred every 10th generation to prevent genetic drift as recommended by The Jackson Laboratory. All mice were fed PicoLab Rodent Diet 5LOD (standard diet, or SD) containing 240 ppm iron, provided by the Department of Comparative Medicine, Oregon Health and Science University, until 4–5 weeks of age. The mice were then transferred to either a synthetic control diet (CD), containing 287 ppm iron, or an iron-deficient diet consisting of 2–6 parts/million Fe (Envigo Teklad TD.09488 and TD.08714, respectively). Mice were maintained on their respective diets for the duration of the experiment. Although the mice used in this study had a RBC count, Hb, and hematocrit lower than previously reported (57), this decrease was not caused by use of synthetic diets because mice fed a SD had similar blood profiles to those fed a CD (Table S2 and Fig. S5). All data are from male mice between 9 and 12 weeks of age.

Tissue isolation

For nonterminal assays, blood was obtained by retro-orbital puncture from mice anesthetized with isoflurane (Piramal Enterprise). For terminal assays, blood was obtained through the inferior vena cava of mice anesthetized by administering an intraperitoneal injection containing 100 mg of ketamine (Par Pharmaceutical), 15 mg of xylazine (Lloyd Laboratories), and 5 mg of acepromazine maleate (Henry Schein Animal Health) per kg of body mass. Blood was collected in EDTA-treated tubes (Sarstedt) for flow cytometry analyses. Serum was isolated from untreated, circulating blood that was coagulated at room temperature for 2 h and centrifuged at 2000 $\times$ *g* for 20 min.

For protein analyses, spleens were excised, snap-frozen in liquid nitrogen, and stored at −80 °C. For flow cytometry analyses, spleen and femoral BM were isolated in Hanks' balanced salt solution (HBSS) modified with 3% fetal bovine serum and 10 mM HEPES (Sigma). Spleens were pressed through a 70-μm filter (Thermo Fisher Scientific), and both splenic and BM cells were then strained through a 35-μm filter (BD Biosciences). Nucleated cell concentration was determined by lysing RBCs and staining nuclei with Türk solution (0.01% crystal violet, 1% glacial acetic acid) followed by quantification with a hemocytometer.

Liver-specific gene expression

Preparation and administration of the serotype 2 adeno-associated viral vector containing the full-length mouse *Tfr2* ORF

under the regulation of a hepatocyte-specific promoter and pseudo-typed with the serotype 8 capsid (AAV2/8-*Tfr2*) was performed as described previously (37). Briefly, 8-week-old male mice were injected with either 200 μl of PBS or 200 μl of PBS containing 1.6×10^{12} viral genome equivalents of AAV2/8-*Tfr2* via the tail vein. Three weeks later, mice were euthanized, and tissue was harvested for analysis.

EPO ELISA

Serum EPO levels were evaluated using the Mouse Erythropoietin Quantikine ELISA kit according to the manufacturer's protocol (R&D Systems).

Hematopoietic colony-forming cell assay

For quantification of the BFU-E population density, 6×10^4 and 3×10^5 respective amounts of nucleated BM and spleen cells were plated in 1 ml of methylcellulose complete medium containing 50 ng/ml recombinant human SCF, 10 ng/ml rmIL-3, 10 ng/ml rmIL-6, and 5 IU/ml rmEPO (R&D Systems). For CFU-E analysis, 2×10^5 nucleated BM and 10^6 nucleated spleen cells were plated. Colonies formed from CFU-E and BFU-E progenitor cells were analyzed 2 and 10 days after plating, respectively. Colonies formed from erythroid lineage progenitor cells were distinguished by the addition of a 1-ml solution containing 0.2% benzidine dihydrochloride and 3% H_2O_2 in 0.5 M acetic acid (Sigma).

Flow cytometry and cell sorting

Complete blood count was measured directly from EDTA-treated blood samples using a Hemavet 950FS (Drew Scientific). All other flow cytometry analyses were performed using a FacsCanto II cytometer or Influx cell sorter (BD Biosciences).

For circulating reticulocyte analysis, 5 μl of EDTA-treated peripheral blood was added to a 1-ml PBS solution containing 0.1 μg/ml thiazole orange, 0.002 M EDTA, and 0.002% NaN_3 (Sigma) and stained for 30 min at room temperature in the dark.

All fluorescently labeled antibodies were purchased from eBioscience. For erythroid lineage analysis, cells were labeled with anti-human/mouse CD44-FITC (1:200), anti-mouse CD71-PE (1:400), and anti-mouse Terr119-PECy7 (1:100). For the purpose of excluding nonerythroid lineage cells, the following antibodies were added: anti-mouse CD11b(Mac1)-APC (1:100), anti-human/mouse CD45R(B220)-APC (1:200), and anti-mouse Ly-6G-APC (1:200). Cells were stained in the aforementioned modified HBSS at a concentration of 10^6 nucleated cells/100 μl for 30 min at room temperature in the dark. Propidium iodide (PI, 1 μg/ml) was added directly before analysis for dead cell exclusion. Erythroid populations were quantified by sorting a total of 10^5 events for the BM or 1.2×10^6 events for the spleen.

qRT-PCR

RNA was extracted from isolated erythroid populations using NucleoSpin RNA kit (Macherey-Nagel). Moloney murine leukemia virus reverse transcriptase and a combination of random hexamers with oligo$(dT)_{12-18}$ primers (Invitrogen) were used for first-strand cDNA synthesis. Quantification of cDNA was determined on a ViiA 7 real-time PCR system using SYBR Green Master Mix (Applied Biosystems) and the primers listed in Table S3. Data were analyzed using the comparative C_t method, and are represented as fold change in ΔC_t.

Serum and nonheme iron assay

Serum iron concentration and Tf saturation were evaluated using an iron/TIBC reagent set (Pointe Scientific) according to the manufacturer's protocol. Liver tissue was digested and analyzed as described previously (58).

Western blot analysis

Western blotting assays were performed as described previously (59). In brief, cells were lysed on ice in NET-Triton X-100 buffer (150 mM NaCl, 5 mM EDTA, 10 mM Tris, pH 7.4, 1% Triton X-100) containing 1× Complete Mini Protease Inhibitor Mixture (Roche Diagnostics). Lysates were cleared by centrifugation at 15,000 × *g* for 10 min. Protein concentration was measured using the BCA Protein Assay (Pierce). Volumes containing 100 μg of total protein were analyzed for each sample. Polyclonal rabbit anti-TFR2 serum was produced at Pocono Rabbit Farm and Laboratory (Canadensis, PA) by immunizing rabbits with purified TFR2 ectodomain. The specificity of the rabbit anti-TFR2 serum was verified in the manner described for the 9F81C11 mouse anti-TFR2 antibody (60). Monoclonal mouse anti-ACTB was obtained from Proteintech. Secondary antibodies against rabbit and mouse (IgG) conjugated to horseradish peroxidase were purchased from Millipore Sigma.

Statistical analyses

All data are presented as mean ± S.D. of the indicated number of biological replicates. Statistically significant differences were determined using one- or two-way ANOVA, followed by Tukey's multiple comparison test or Fisher's LSD test as indicated (GraphPad Prism).

Author contributions—A. M. W., D. C. G., J. C., W. H. F., A.-S. Z., and C. A. E. conceptualization; A. M. W. and J. C. data curation; A. M. W., D. C. G., and C. A. E. formal analysis; A. M. W., J. C., and C. A. E. methodology; A. M. W., D. C. G., J. C., W. H. F., A.-S. Z., and C. A. E. writing-review and editing; D. C. G. and C. A. E. supervision; C. A. E. funding acquisition; C. A. E. investigation; C. A. E. writing-original draft; C. A. E. project administration.

Acknowledgments—We thank Drs. Shelley S. Mason and Christal A. Worthen for the preliminary results on the project, and James Cahill and Katie Kulp for technical assistance.

References

1. Pietrangelo, A. (2010) Hereditary hemochromatosis: pathogenesis, diagnosis, and treatment. *Gastroenterology* **139,** 393–408.e1–2 CrossRef Medline
2. Santos, P. C., Krieger, J. E., and Pereira, A. C. (2012) Molecular diagnostic and pathogenesis of hereditary hemochromatosis. *Int. J. Mol. Sci.* **13,** 1497–1511 CrossRef Medline
3. Crownover, B. K., and Covey, C. J. (2013) Hereditary hemochromatosis. *Am. Fam. Physician* **87,** 183–190 Medline
4. Salgia, R. J., and Brown, K. (2015) Diagnosis and management of hereditary hemochromatosis. *Clin. Liver Dis.* **19,** 187–198 CrossRef Medline
5. Kawabata, H., Yang, R., Hirama, T., Vuong, P. T., Kawano, S., Gombart, A. F., and Koeffler, H. P. (1999) Molecular cloning of transferrin receptor

2 a new member of the transferrin receptor-like family. *J. Biol. Chem.* **274,** 20826–20832 CrossRef Medline
6. Kawabata, H., Germain, R. S., Ikezoe, T., Tong, X., Green, E. M., Gombart, A. F., and Koeffler, H. P. (2001) Regulation of expression of murine transferrin receptor 2. *Blood* **98,** 1949–1954 CrossRef Medline
7. Chloupková, M., Zhang, A.-S., and Enns, C. A. (2010) Stoichiometries of transferrin receptors 1 and 2 in human liver. *Blood Cells Mol. Dis.* **44,** 28–33 CrossRef Medline
8. Wallace, D. F., Summerville, L., and Subramaniam, V. N. (2007) Targeted disruption of the hepatic transferrin receptor 2 gene in mice leads to iron overload. *Gastroenterology* **132,** 301–310 CrossRef Medline
9. Fillebeen, C., Charlebois, E., Wagner, J., Katsarou, A., Mui, J., Vali, H., Garcia-Santos, D., Ponka, P., Presley, J., and Pantopoulos, K. (2019) Transferrin receptor 1 controls systemic iron homeostasis by fine-tuning hepcidin expression to hepatocellular iron load. *Blood* **133,** 344–355 CrossRef Medline
10. Fleming, R. E., Migas, M. C., Holden, C. C., Waheed, A., Britton, R. S., Tomatsu, S., Bacon, B. R., and Sly, W. S. (2000) Transferrin receptor 2: continued expression in mouse liver in the face of iron overload and in hereditary hemochromatosis. *Proc. Natl. Acad. Sci. U.S.A.* **97,** 2214–2219 CrossRef Medline
11. Johnson, M. B., and Enns, C. A. (2004) Diferric transferrin regulates transferrin receptor 2 protein stability. *Blood* **104,** 4287–4293 CrossRef Medline
12. Johnson, M. B., Chen, J., Murchison, N., Green, F. A., and Enns, C. A. (2007) Transferrin receptor 2: evidence for ligand-induced stabilization and redirection to a recycling pathway. *Mol. Biol. Cell* **18,** 743–754 CrossRef Medline
13. Chen, J., Wang, J., Meyers, K. R., and Enns, C. A. (2009) Transferrin-directed internalization and cycling of transferrin receptor 2. *Traffic* **10,** 1488–1501 CrossRef Medline
14. Pagani, A., Vieillevoye, M., Nai, A., Rausa, M., Ladli, M., Lacombe, C., Mayeux, P., Verdier, F., Camaschella, C., and Silvestri, L. (2015) Regulation of cell surface transferrin receptor-2 by iron-dependent cleavage and release of a soluble form. *Haematologica.* **100,** 458–465 CrossRef Medline
15. Camaschella, C., Roetto, A., Calì, A., De Gobbi, M., Garozzo, G., Carella, M., Majorano, N., Totaro, A., and Gasparini, P. (2000) The gene *TFR2* is mutated in a new type of haemochromatosis mapping to 7q22. *Nat. Genet.* **25,** 14–15 CrossRef Medline
16. Joshi, R., Shvartsman, M., Morán, E., Lois, S., Aranda, J., Barqué, A., de la Cruz, X., Bruguera, M., Vagace, J. M., Gervasini, G., Sanz, C., and Sánchez, M. (2015) Functional consequences of transferrin receptor-2 mutations causing hereditary hemochromatosis type 3. *Mol. Genet. Genomic Med.* **3,** 221–232 CrossRef Medline
17. Fleming, R. E., Ahmann, J. R., Migas, M. C., Waheed, A., Koeffler, H. P., Kawabata, H., Britton, R. S., Bacon, B. R., and Sly, W. S. (2002) Targeted mutagenesis of the murine transferrin receptor-2 gene produces hemochromatosis. *Proc. Natl. Acad. Sci. U.S.A.* **99,** 10653–10658 CrossRef Medline
18. Drake, S. F., Morgan, E. H., Herbison, C. E., Delima, R., Graham, R. M., Chua, A. C., Leedman, P. J., Fleming, R. E., Bacon, B. R., Olynyk, J. K., and Trinder, D. (2007) Iron absorption and hepatic iron uptake are increased in a transferrin receptor 2 (Y245X) mutant mouse model of hemochromatosis type 3. *Am. J. Physiol. Gastrointest. Liver Physiol.* **292,** G323–G328 CrossRef Medline
19. Kawabata, H., Fleming, R. E., Gui, D., Moon, S. Y., Saitoh, T., O'Kelly, J., Umehara, Y., Wano, Y., Said, J. W., and Koeffler, H. P. (2005) Expression of hepcidin is down-regulated in TfR2 mutant mice manifesting a phenotype of hereditary hemochromatosis. *Blood* **105,** 376–381 CrossRef Medline
20. Nestorowa, S., Hamey, F. K., Pijuan Sala, B., Diamanti, E., Shepherd, M., Laurenti, E., Wilson, N. K., Kent, D. G., and Göttgens, B. (2016) A single-cell resolution map of mouse hematopoietic stem and progenitor cell differentiation. *Blood* **128,** e20–e31 CrossRef Medline
21. Nai, A., Lidonnici, M. R., Rausa, M., Mandelli, G., Pagani, A., Silvestri, L., Ferrari, G., and Camaschella, C. (2015) The second transferrin receptor regulates red blood cell production in mice. *Blood* **125,** 1170–1179 CrossRef Medline
22. Rishi, G., Secondes, E. S., Wallace, D. F., and Subramaniam, V. N. (2016) Hematopoietic deletion of transferrin receptor 2 in mice leads to a block in erythroid differentiation during iron-deficient anemia. *Am. J. Hematol.* **91,** 812–818 CrossRef Medline
23. Forejtnikovà, H., Vieillevoye, M., Zermati, Y., Lambert, M., Pellegrino, R. M., Guihard, S., Gaudry, M., Camaschella, C., Lacombe, C., Roetto, A., Mayeux, P., and Verdier, F. (2010) Transferrin receptor 2 is a component of the erythropoietin receptor complex and is required for efficient erythropoiesis. *Blood* **116,** 5357–5367 CrossRef Medline
24. Chen, K., Liu, J., Heck, S., Chasis, J. A., An, X., and Mohandas, N. (2009) Resolving the distinct stages in erythroid differentiation based on dynamic changes in membrane protein expression during erythropoiesis. *Proc. Natl. Acad. Sci. U.S.A.* **106,** 17413–17418 CrossRef Medline
25. Liu, J., Zhang, J., Ginzburg, Y., Li, H., Xue, F., De Franceschi, L., Chasis, J. A., Mohandas, N., and An, X. (2013) Quantitative analysis of murine terminal erythroid differentiation *in vivo*: novel method to study normal and disordered erythropoiesis. *Blood* **121,** e43–e49 CrossRef Medline
26. Doty, R. T., Phelps, S. R., Shadle, C., Sanchez-Bonilla, M., Keel, S. B., and Abkowitz, J. L. (2015) Coordinate expression of heme and globin is essential for effective erythropoiesis. *J. Clin. Invest.* **125,** 4681–4691 CrossRef Medline
27. Heath, D. S., Axelrad, A. A., McLeod, D. L., and Shreeve, M. M. (1976) Separation of the erythropoietin-responsive progenitors BFU-E and CFU-E in mouse bone marrow by unit gravity sedimentation. *Blood* **47,** 777–792 CrossRef Medline
28. Hu, J., Liu, J., Xue, F., Halverson, G., Reid, M., Guo, A., Chen, L., Raza, A., Galili, N., Jaffray, J., Lane, J., Chasis, J. A., Taylor, N., Mohandas, N., and An, X. (2013) Isolation and functional characterization of human erythroblasts at distinct stages: implications for understanding of normal and disordered erythropoiesis *in vivo*. *Blood* **121,** 3246–3253 CrossRef Medline
29. Rauner, M., Baschant, U., Roetto, A., Pellegrino, R. M., Rother, S., Salbach-Hirsch, J., Weidner, H., Hintze, V., Campbell, G., Petzold, A., Lemaitre, R., Henry, I., Bellido, T., Theurl, I., Altamura, S., *et al.* (2019) Transferrin receptor 2 controls bone mass and pathological bone formation via BMP and Wnt signalling. *Nat. Metab.* **1,** 111–124 CrossRef Medline
30. Landschulz, K. T., Boyer, S. H., Noyes, A. N., Rogers, O. C., and Frelin, L. P. (1992) Onset of erythropoietin response in murine erythroid colony-forming units: assignment to early S-phase in a specific cell generation. *Blood* **79,** 2749–2758 CrossRef Medline
31. Koulnis, M., Porpiglia, E., Hidalgo, D., and Socolovsky, M. (2014) Erythropoiesis: from molecular pathways to system properties. *Adv. Exp. Med. Biol.* **844,** 37–58 CrossRef Medline
32. Oshima, K., Ikeda, Y., Horinouchi, Y., Watanabe, H., Hamano, H., Kihira, Y., Kishi, S., Izawa-Ishizawa, Y., Miyamoto, L., Hirayama, T., Nagasawa, H., Ishizawa, K., Tsuchiya, K., and Tamaki, T. (2017) Iron suppresses erythropoietin expression via oxidative stress-dependent hypoxia-inducible factor-2α inactivation. *Lab. Invest.* **97,** 555–566 CrossRef Medline
33. Wallerstein, R. O. (1987) Laboratory evaluation of anemia. *West. J. Med.* **146,** 443–451 Medline
34. Bessman, J. D., Gilmer, P. R., Jr., and Gardner, F. H. (1983) Improved classification of anemias by MCV and RDW. *Am. J. Clin. Pathol.* **80,** 322–326 CrossRef Medline
35. Johnson, C. S., Tegos, C., and Beutler, E. (1983) Thalassemia minor: routine erythrocyte measurements and differentiation from iron deficiency. *Am. J. Clin. Pathol.* **80,** 31–36 CrossRef Medline
36. Grover, A., Mancini, E., Moore, S., Mead, A. J., Atkinson, D., Rasmussen, K. D., O'Carroll, D., Jacobsen, S. E., and Nerlov, C. (2014) Erythropoietin guides multipotent hematopoietic progenitor cells toward an erythroid fate. *J. Exp. Med.* **211,** 181–188 CrossRef Medline
37. Gao, J., Chen, J., De Domenico, I., Koeller, D. M., Harding, C. O., Fleming, R. E., Koeberl, D. D., and Enns, C. A. (2010) Hepatocyte-targeted HFE and TFR2 control hepcidin expression in mice. *Blood* **115,** 3374–3381 CrossRef Medline
38. Kleven, M. D., Gomes, M. M., Wortham, A. M., Enns, C. A., and Kahl, C. A. (2018) Ultrafiltered recombinant AAV8 vector can be safely administered *in vivo* and efficiently transduces liver. *PLoS ONE* **13,** e0194728 CrossRef Medline

39. Kautz, L., Jung, G., Valore, E. V., Rivella, S., Nemeth, E., and Ganz, T. (2014) Identification of erythroferrone as an erythroid regulator of iron metabolism. *Nat. Genet.* **46,** 678–684 CrossRef Medline
40. Kautz, L., Jung, G., Nemeth, E., and Ganz, T. (2014) Erythroferrone contributes to recovery from anemia of inflammation. *Blood* **124,** 2569–2574 CrossRef Medline
41. Jiang, X., Gao, M., Chen, Y., Liu, J., Qi, S., Ma, J., Zhang, Z., and Xu, Y. (2016) EPO-dependent induction of erythroferrone drives hepcidin suppression and systematic iron absorption under phenylhydrazine-induced hemolytic anemia. *Blood Cells Mol. Dis.* **58,** 45–51 CrossRef Medline
42. Roetto, A., Di Cunto, F., Pellegrino, R. M., Hirsch, E., Azzolino, O., Bondi, A., Defilippi, I., Carturan, S., Miniscalco, B., Riondato, F., Cilloni, D., Silengo, L., Altruda, F., Camaschella, C., and Saglio, G. (2010) Comparison of 3 Tfr2-deficient murine models suggests distinct functions for Tfr2-α and Tfr2-β isoforms in different tissues. *Blood* **115,** 3382–3389 CrossRef Medline
43. Nai, A., Pellegrino, R. M., Rausa, M., Pagani, A., Boero, M., Silvestri, L., Saglio, G., Roetto, A., and Camaschella, C. (2014) The erythroid function of transferrin receptor 2 revealed by *Tmprss6* inactivation in different models of transferrin receptor 2 knockout mice. *Haematologica* **99,** 1016–1021 CrossRef Medline
44. Wallace, D. F., Secondes, E. S., Rishi, G., Ostini, L., McDonald, C. J., Lane, S. W., Vu, T., Hooper, J. D., Velasco, G., Ramsay, A. J., Lopez-Otin, C., and Subramaniam, V. N. (2015) A critical role for murine transferrin receptor 2 in erythropoiesis during iron restriction. *Br. J. Haematol.* **168,** 891–901 CrossRef Medline
45. Schmidt, P. J., and Fleming, M. D. (2012) Transgenic HFE-dependent induction of hepcidin in mice does not require transferrin receptor-2. *Am. J. Hematol.* **87,** 588–595 CrossRef Medline
46. Fleming, R. E., Holden, C. C., Tomatsu, S., Waheed, A., Brunt, E. M., Britton, R. S., Bacon, B. R., Roopenian, D. C., and Sly, W. S. (2001) Mouse strain differences determine severity of iron accumulation in Hfe knockout model of hereditary hemochromatosis. *Proc. Natl. Acad. Sci. U.S.A.* **98,** 2707–2711 CrossRef Medline
47. Ramos, E., Kautz, L., Rodriguez, R., Hansen, M., Gabayan, V., Ginzburg, Y., Roth, M.-P., Nemeth, E., and Ganz, T. (2011) Evidence for distinct pathways of hepcidin regulation by acute and chronic iron loading. *Hepatology* **53,** 1333–1341 CrossRef Medline
48. Leonard, J. P., May, W. S., Ihle, J. N., Pettit, G. R., and Sharkis, S. J. (1988) Regulation of hematopoiesis-IV: the role of interleukin-3 and bryostatin 1 in the growth of erythropoietic progenitors from normal and anemic W/Wv mice. *Blood* **72,** 1492–1496 CrossRef Medline
49. Socolovsky, M., Fallon, A. E., and Lodish, H. F. (1998) The prolactin receptor rescues EpoR$^{-/-}$ erythroid progenitors and replaces EpoR in a synergistic interaction with c-kit. *Blood* **92,** 1491–1496 CrossRef Medline
50. Terszowski, G., Waskow, C., Conradt, P., Lenze, D., Koenigsmann, J., Carstanjen, D., Horak, I., and Rodewald, H.-R. (2005) Prospective isolation and global gene expression analysis of the erythrocyte colony-forming unit (CFU-E). *Blood* **105,** 1937–1945 CrossRef Medline
51. Li, J., Hale, J., Bhagia, P., Xue, F., Chen, L., Jaffray, J., Yan, H., Lane, J., Gallagher, P. G., Mohandas, N., Liu, J., and An, X. (2014) Isolation and transcriptome analyses of human erythroid progenitors: BFU-E and CFU-E. *Blood* **124,** 3636–3645 CrossRef Medline
52. Storti, F., Santambrogio, S., Crowther, L. M., Otto, T., Abreu-Rodríguez, I., Kaufmann, M., Hu, C.-J., Dame, C., Fandrey, J., Wenger, R. H., and Hoogewijs, D. (2014) A novel distal upstream hypoxia response element regulating oxygen-dependent erythropoietin gene expression. *Haematologica* **99,** e45–e48 CrossRef Medline
53. Hirano, I., Suzuki, N., Yamazaki, S., Sekine, H., Minegishi, N., Shimizu, R., and Yamamoto, M. (2017) Renal anemia model mouse established by transgenic rescue with an erythropoietin gene lacking kidney-specific regulatory elements. *Mol. Cell. Biol.* **37,** e00451-16 CrossRef Medline
54. Kim, A., and Nemeth, E. (2015) New insights into iron regulation and erythropoiesis. *Curr. Opin. Hematol.* **22,** 199–205 CrossRef Medline
55. Ghosh, M. C., Zhang, D.-L., Jeong, S. Y., Kovtunovych, G., Ollivierre-Wilson, H., Noguchi, A., Tu, T., Senecal, T., Robinson, G., Crooks, D. R., Tong, W.-H., Ramaswamy, K., Singh, A., Graham, B. B., Tuder, R. M., *et al.* (2013) Deletion of iron regulatory protein 1 causes polycythemia and pulmonary hypertension in mice through translational derepression of HIF2α. *Cell Metab.* **17,** 271–281 CrossRef Medline
56. Anderson, S. A., Nizzi, C. P., Chang, Y.-I., Deck, K. M., Schmidt, P. J., Galy, B., Damnernsawad, A., Broman, A. T., Kendziorski, C., Hentze, M. W., Fleming, M. D., Zhang, J., and Eisenstein, R. S. (2013) The IRP1-HIF-2α axis coordinates iron and oxygen sensing with erythropoiesis and iron absorption. *Cell Metab.* **17,** 282–290 CrossRef Medline
57. Kile, B. T., Mason-Garrison, C. L., and Justice, M. J. (2003) Sex and strain-related differences in the peripheral blood cell values of inbred mouse strains. *Mamm. Genome* **14,** 81–85 CrossRef Medline
58. Wahedi, M., Wortham, A. M., Kleven, M. D., Zhao, N., Jue, S., Enns, C. A., and Zhang, A.-S. (2017) Matriptase-2 suppresses hepcidin expression by cleaving multiple components of the hepcidin induction pathway. *J. Biol. Chem.* **292,** 18354–18371 CrossRef Medline
59. Chen, J., and Enns, C. A. (2007) The cytoplasmic domain of transferrin receptor 2 dictates its stability and response to Holo-transferrin in Hep3B cells. *J. Biol. Chem.* **282,** 6201–6209 CrossRef Medline
60. Vogt, T. M., Blackwell, A. D., Giannetti, A. M., Bjorkman, P. J., and Enns, C. A. (2003) Heterotypic interactions between transferrin receptor and transferrin receptor 2. *Blood* **101,** 2008–2014 CrossRef Medline